

#478

VOYAGER 1 + 2

PLANETARY RADIO ASTRONOMY DATA

77-084A-10C
77-076A-10C

VOYAGER 1

PLANET RADIO ASST (PRA)

77-084A-10C

THIS DATA SET HAS BEEN RESTORED. THERE WERE ORIGINALLY FOUR 9-TRACK, 6250 BPI TAPES, WRITTEN IN BINARY. THERE ARE FOUR RESTORED TAPES. THE DR TAPES ARE 3480 CARTRIDGES AND THE DS TAPES ARE 9-TRACK, 6250 BPI. THE ORIGINAL TAPES WERE CREATED ON AN IBM 360 COMPUTER. THE DR AND DS NUMBERS ALONG WITH THE CORRESPONDING D NUMBERS AND TIME SPANS ARE AS FOLLOWS:

DR#	DS#	DD#	FILES	TIME SPAN
DR004181	DS004181	D043048	1	09/05/77 - 06/30/78
DR004182	DS004182	D043049	1	07/26/78 - 02/28/79
DR004183	DS004183	D043050	1	03/01/79 - 07/18/79
DR004184	DS004184	D043051	1	08/02/79 - 03/31/80

VOYAGER 2

PLANETARY RADIO ASTRONOMY DATA

77-076A-10C

THIS DATA SET HAS BEEN RESTORED. ORIGINALLY IT CONTAINED FOUR 9-TRACK, 6250 BPI TAPES WRITTEN IN BINARY. THERE ARE TWO RESTORED TAPES. THE DR TAPES ARE 3480 CARTRIDGES AND THE DS TAPES ARE 9-TRACK, 6250 BPI. THE ORIGINAL TAPE WERE CREATED ON AN IBM 360 COMPUTER AND THEY WERE RESTORED ON THE MRS SYSTEM. THE DR AND DS NUMBERS ALONG WITH THE CORRESPONDING D NUMBERS AND THE TIME SPANS ARE AS FOLLOWS:

DR#	DS#	D#	FILES	TIME SPAN
DR004225	DS004225	D043052 D043053	1 2	08/20/77 - 06/20/78 07/25/78 - 05/31/79
DR004226	DS004226	D043054 D043055	1 2	06/01/79 - 08/10/79 08/19/79 - 04/30/80

REQ. AGENT
BER

RAND NO.
VOO

ACQ. AGENT
RWV

VOYAGER 1 & 2

PLANETARY RADIO ASTRONOMY DATA

77-084A-10C

77-076A-10C

This data set catalog consist of 4 Voyager 1 and 4 Voyager 2 data tapes covering the Jupiter encounters. The data tapes are 6250 BPI, Binary, 9-track and containing one file of data each. The tapes were created on an IBM 360 computer.

The time spans are as follows:

Voyager 1

<u>D#</u>	<u>C#</u>	<u>TIME SPANS</u>
D-43048	C-21295	09/05/77 - 06/30/78
D-43049	C-21296	07/26/78 - 02/28/79
D-43050	C-21297	03/01/79 - 07/26/79
D-43051	C-21298	08/02/79 - 03/31/80

Voyager 2

<u>D#</u>		
D-43052	C-21299	08/20/77 - 06/20/78
D-43053	C-21300	07/25/78 - 05/31/79
D-43054	C-21301	06/01/79 - 08/10/79
D-43055	C-21302	08/19/79 - 04/30/80

77-084A-10C

B35770-00A

ORI

Silver Spring, Maryland 20910

VOYAGER PLANETARY RADIO ASTRONOMY
EXPERIMENT DATA DESCRIPTION

SEPTEMBER, 1980

PREPARED FOR
NATIONAL AERONAUTICS AND SPACE ADMINISTRATION
GODDARD SPACE FLIGHT CENTER
GREENBELT, MARYLAND 20771

TABLE OF CONTENTS

	<u>PAGE</u>
LIST OF TABLES	ii
LIST OF FIGURES	ii
ABSTRACT	1
INSTRUMENT DESCRIPTION	2
OPERATING MODES	8
DATA DESCRIPTION	12
DYNAMIC SPECTRA PLOTS	28
PRA PUBLICATIONS	32
PRA BIBLIOGRAPHY	34

LIST OF TABLES

TABLE	TITLE	<u>PAGE</u>
1.	PRA Experiment Salient Information	3
2.	Voyager 1 and 2 Events	13
3.	Table Index Mode Mix Interpretation	19
4.	Cruise Mode Data Rates	21
5.	Voyager Frame Averages Tapes	26
6.	Frame Averages Tape Volumes.	27
A-1	Voyager Antenna Angles	37
A-2	PRA Receiver Frequencies	42

LIST OF FIGURES

FIGURE	TITLE	<u>PAGE</u>
1.	Major Voyager Spacecraft Systems	4
2.	Block Diagram of PRA Receiver	5
3.	PRA Antenna Orientation.	6
4.	Plot of Cruise Mode Changes	22
5.	Flow of Data from Voyager to GSFC	23
6.	Flow of Data Processing at GSFC.	25
7.	Low-Band, 24-hour Dynamic Spectra Plot	29
8.	High-Band, 24-hour Dynamic Spectra Plot	30
9.	"Ghost" Signals in Dynamic Spectra Plot.	31

ABSTRACT

This document is intended as an introductory manual for the use of the Voyager Planetary Radio Astromony (PRA) data stored at the National Space Science Data Center (NSSDC). It includes a brief description of the PRA receiver electronics and the programmable modes in which it can operate. The frame-averaged, millibel tapes and the 24-hour dynamic spectra plots which are immediately available through the NSSDC are explained. Finally, the publications which have resulted from the PRA data through 1979 are listed.

INSTRUMENT DESCRIPTION

The following is a brief summary of the characteristics of the PRA instrumentation. A more detailed description can be found in Lang and Peltzer (1977) and Warwick et al. (1977). The salient characteristics are summarized in Table 1.

Both Voyager spacecraft carry identical radiometers consisting of two orthogonal ten meter monopoles (Figure 1) coupled to individual pre-amplifiers and mixers. The mixer outputs are then fed to a 90° hybrid followed by parallel IF amplifiers (Figure 2). This allows the system to measure the left-hand (LH) and right-hand (RH) circularly polarized components of the wave, but not its linear components or the phase difference between the components. This is equivalent to measuring only two of the four Stokes parameters necessary to completely define the wave polarization state. Thus, only the total power and polarization sense of the wave, either LH or RH depending on which signal is stronger, can be determined unambiguously from a single measurement. This determination alone is invaluable in helping to specify source locations and emission modes and in distinguishing one emission source from another.

In many cases the degree of polarization can be bounded based on the polarization measurements and knowledge of the angle between the direction normal to the antenna plane and the source of emission. The antenna plane is defined by the plane of the two monopoles and is oriented relative to the rest of the spacecraft as shown in Figure 3. Table A-1 displays the antenna normal angle relative to Jupiter for the two Voyagers. The values are extracted from the Voyager ephemeris tapes. Whenever the angle changes by more than 1° a new value is tabulated. Thus, in times of frequent spacecraft maneuvering a large number of entries appear. In studies of the polarization of the data, Table A-1 should be consulted since the sign of the polarization should not be trusted when the antenna normal angle is within 35° of 90° .

At low frequencies (around 3 MHz), each monopole antenna is substantially shorter than one wavelength and, in effect, has the small radiation resistance and isotropic reception pattern of a Hertzian dipole. At

TABLE 1

PRA EXPERIMENT SALIENT INFORMATION

Receiver

Low Frequency Band	70 channels
Frequency Range	1.2 kHz - 1326 kHz
Bandwidth.	1 kHz
Frequency Spacing.	19.2 kHz
Sensitivity.	0.3 μ V/ $\sqrt{\text{kHz}}$
High Frequency Band.	128 channels
Frequency Range.	1.2 MHz - 40.5 MHz
Bandwidth.	200 kHz
Frequency Spacing.	307.2 kHz
Sensitivity.	0.1 μ V/ $\sqrt{\text{kHz}}$
Dynamic Range (with commandable attenuators) .	140 dB
Dynamic Range (for fixed attenuation)	50 dB

Operating Modes

POLLO, HARAD, LEVEL, FIXLO

Frequency Range Scan Time.	6 sec
Postdetection Time Constant.	25 msec
Frequency Synthesizer Settling Time. .	5 msec
Data Rate (Maximum).	266 $2/3$ bps

PHIEX

Postdetection Time Constant.	0.1 ms
Data Rate.	115.2 kbps

POLHI

Postdetection Time Constant.	0.1 msec
Data Rate (Maximum).	266 $2/3$ bps

Antennas

Length	10 m
Effective Area (Low band wavelengths only (λ))	$0.119 \lambda^2$

Principal Investigator

J.W. Warwick, Radiophysics, Inc., Boulder, CO 80301

Deputy Principal Investigator

J.K. Alexander, Goddard Space Flight Center, Greenbelt, MD 20771

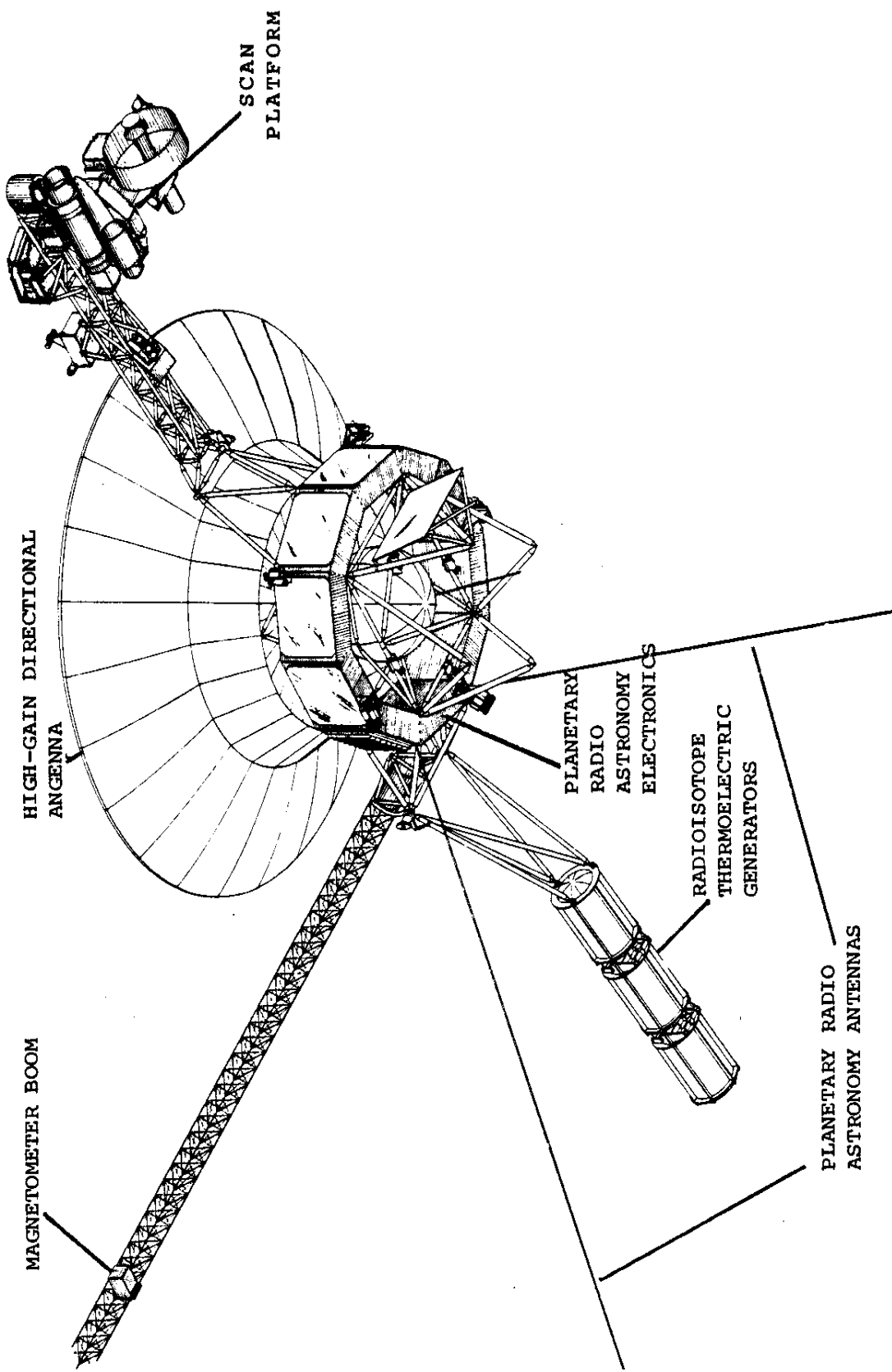


FIGURE 1. Diagram of the Voyager spacecraft showing the Planetary Radio Astronomy antennas and electronics and other spacecraft components.

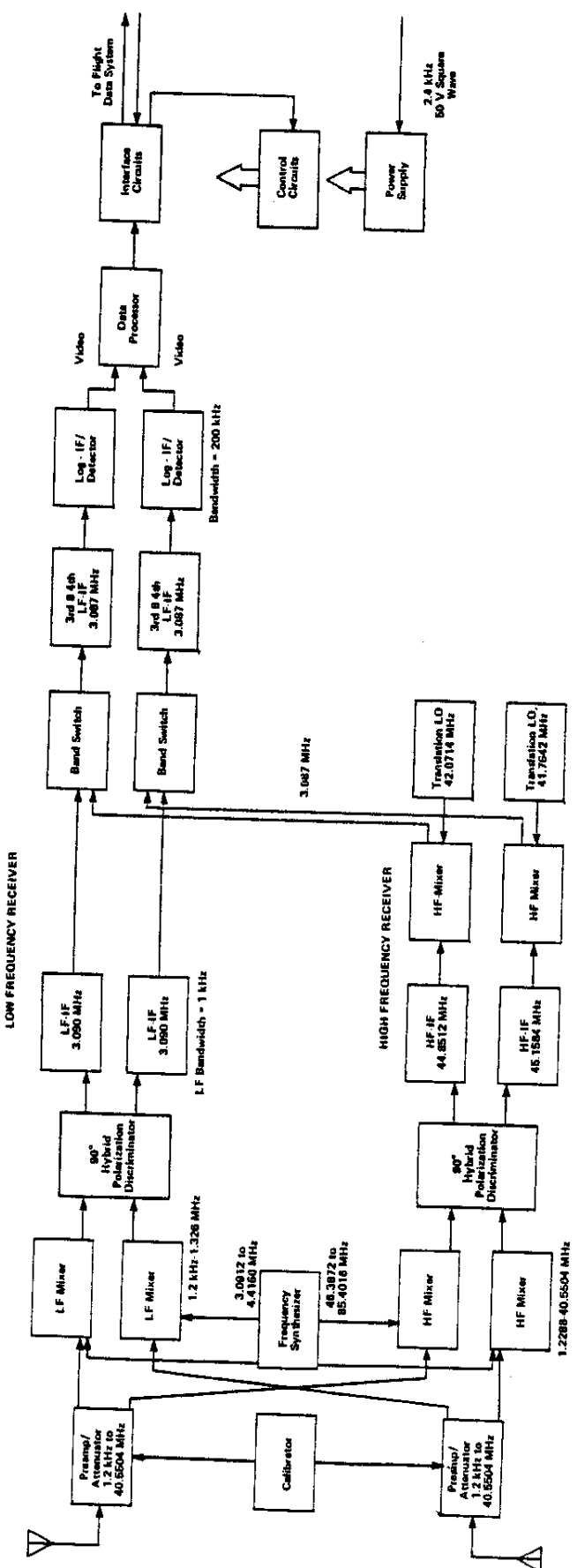


FIGURE 2. Simplified block diagram of the PRA receiver electronics.

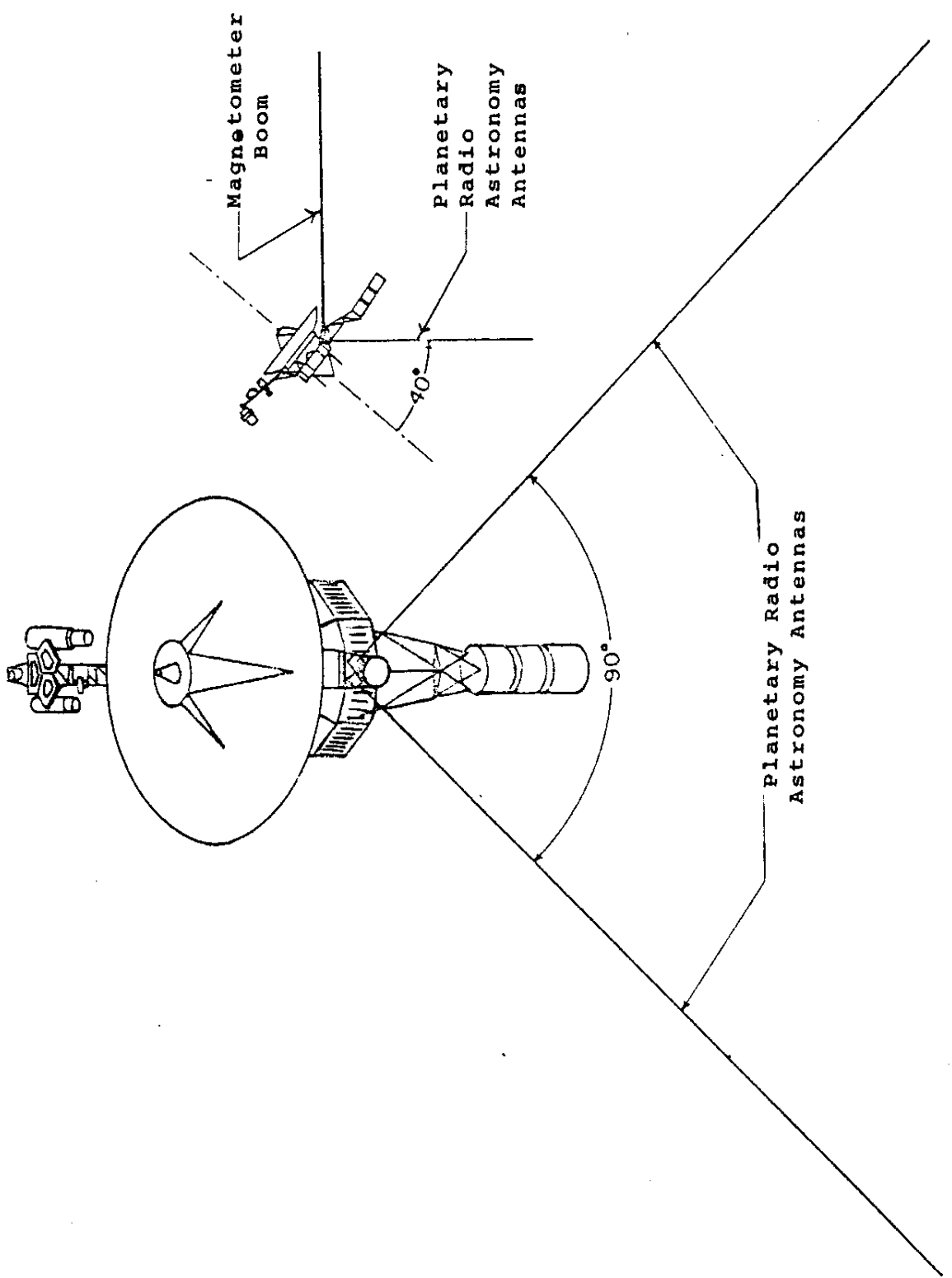


FIGURE 3. Simplified diagram of the Voyager Spacecraft showing the orientation of the PRA antennas.

higher frequencies, the pattern becomes multilobed since the antenna elements now must support a more complex current distribution. In actuality, this "utopian" behavior is altered slightly by the presence of the large conducting surfaces near the monopoles. Examples of these conducting surfaces are the 13 meter magnetometer boom and the 3.7 meter diameter high-gain telemetry antenna. Since the low frequency antenna pattern is so simple and since the other spacecraft appendages are all short compared to a wavelength, the low-frequency observations appear to have been affected the least by spacecraft perturbations to the antenna response pattern. At higher frequencies, complete reversals in the polarization sense from one frequency band to another sometimes appear which are clearly instrumental in origin. The bands of frequencies most often affected are approximately 5 MHz and 15 MHz on both spacecraft. Caution must be exercised in separating instrumental polarization reversals from the true reversals which may be evident near these frequencies.

The PRA receiver operates in two broad frequency bands whose channel bandwidths and separations are different. The 1.2 kHz to 1326 kHz low-frequency (LF) band consists of seventy 1 kHz wide channels, each separated by 19.2 kHz. The 1.2 MHz to 40.5 MHz high-frequency (HF) band consists of 129 channels, each of 200 kHz bandwidth. The separation between channels in the HF band is 307.2 kHz. A complete listing of channel numbers and corresponding frequencies is shown in Table A-2.

The receiver dynamic range expressed logarithmically is 50 dB, and by inserting attenuators in the receiver preamplifiers in anticipation of particularly intense signals, a total effective dynamic range of 140 dB can be achieved. During Voyager 1 (V1) and Voyager 2 (V2) encounters at Jupiter ghost images of intense HF band signals below 10 MHz appeared on some dynamic spectra at 25 MHz and above. These ghost images are due to spurious harmonics generated in the IF section when the high frequency receiver is near saturation. They are for the most part easily identifiable by virtue of their mirror image properties (for example, see Figure 9 around 6 and 18 hours) and are not confused with actual high-frequency decametric emissions.

Although the HF band should in principle be 14 times more sensitive than the LF band in detecting a signal against a uniform background, an extremely high level of noise in the HF band related to Voyager spacecraft high-speed switching logic greatly reduced its effective sensitivity. Thus the HF band observations of Jovian decametric emission (DAM) were limited to the period about one and a half months before and after Jupiter encounter. The excellent spacecraft noise rejection design employed in the LF band permitted detection of Jupiter emission near 1 MHz almost immediately after launch. At V1's closest approach, detection threshold in the PRA LF band was equivalent to $2 \times 10^{-26} \text{ W m}^{-2} \text{ Hz}^{-1}$ if normalized to a distance of 4 A.U. Where the spacecraft noise was the greatest, at 10 MHz in the HF band, the minimum detectable flux from Jupiter was approximately $3 \times 10^{-23} \text{ W m}^{-2} \text{ Hz}^{-1}$. One point worth noting is that toward the high-frequency end of the HF band the detection thresholds are comparable to those found in the LF band. Finally, despite the fact that both V1 and V2 receivers were exposed for a noteworthy length of time to the intense radiation levels in Jupiter's magnetosphere and are approaching their projected four year design lifetimes, no permanent failures have developed and both receivers have performed to their original specifications.

OPERATING MODES

The PRA receiver can be programmed to operate in any of six operational modes. Minor variations in each of these six modes brings the actual number of useful commandable modes to 14. A mode is defined as an instrument and spacecraft Flight Data System (FDS) configuration which produces 200 8-bit words -- 2 words of instrument status followed by 198 data words. The cycle time for a mode is six seconds with one exception to be discussed later. Modes are executed in 48-second frames -- a grouping of eight 200 word records, all in the same mode. The order of execution of the modes is determined from a mode mixture table containing 30 entries, and the modes are commanded in accordance with a continuous cycling through this table. The table can be changed by ground command and has been changed many times in the mission (see Tables 2 and 3).

Although the PRA receiver is capable of being commanded into six basic modes of operation only three of these were used to any large extent in the mission through 1979. These modes are called POLLO, FIXLO, and PHIEX. The modes called POLHI, LEVEL, and HARAD have been used occasionally (see Table 3) but not often enough to warrant detailed discussion. The actual mode in use at any particular time can be determined directly from the status words embedded in each mode scan.

POLLO has been by far the most important data mode in the mission. POLLO is a stepped-frequency mode which samples 198 frequencies in a six second time interval. Sixty msec of each 6-second cycle involves housekeeping chores such as encoding the two 8-bit words describing the status of the experiment. The status words are followed by 198 words of data describing the measurements for each frequency. The signal from each frequency channel is integrated for 25 msec following a 5 msec frequency synthesizer settling time for a total of 30 msec. The receiver then steps to the next lower frequency channel. Only one type of circular polarization is measured with each channel sampling, and this changes in each step. Thus, in one sweep the left-hand polarization of the highest frequency channel is measured followed by the right-hand polarization of the next lower frequency, followed by the left-hand polarization of the channel below that, etc. An exception to this rule, however, is that the polarization measurement does not reverse in the transition from the high band to the low band frequencies. In the next cycle the polarization measurements are reversed and the sweep begins with a measurement of right-hand polarization at the highest frequency. Note that no simultaneous measurements of both polarizations are ever made in POLLO but that measurements can be obtained in opposite polarizations at two adjacent frequencies in 30 msec or at the same frequency in 6 seconds.

POLLO samples 198 frequencies, but there are a total of 199 frequency channels in high and low band which could be sampled. The channel which is not sampled will be either the highest or lowest frequency in high band, depending on the type of POLLO scan implemented. This occurs because the two local oscillator frequencies in high band are offset from each other by 307.2 kHz (see Figure 2) causing a simultaneous measurement of two adjacent frequencies, called the upper and lower channels. In a POLLO sweep all

measurements are made either with the upper channel or the lower channel. If the upper channel is chosen the 128 high band frequencies from 40.5 MHz to 1.5 MHz are sampled. If the sweep uses the lower channel the span of frequencies is from 40.2 MHz to 1.2 MHz. In the data taken through 1979, the POLLO mode sampling the lower channel was used nearly all the time. In low band the two local oscillator frequencies are the same so that all 70 frequency channels are sampled in each POLLO scan.

The FIXLO mode of operation is designed to concentrate the measurements on several frequencies of interest. The output of a FIXLO cycle, like a POLLO cycle, consists of 200 8-bit words of which the first two give information on the status of the instrument. The next 198 words represent measurements made with a continuous repetition of the pattern

$R_L L_L L_U R_U$. R and L are right and left-hand polarization measurements and L and U are the lower and upper channels which are the same in low band, but offset by 307.2 kHz in high band as discussed previously. The FIXLO cycle concentrates on a single frequency (or adjacent frequencies in high band), but three frequencies are sampled in each frame of FIXLO data. If F_1 , F_2 , and F_3 are the three frequencies, then the order in which a FIXLO frame samples them is $F_1 F_2 F_1 F_3 F_1 F_2 F_1 F_3$. Table 2 lists the choice of the three frequencies throughout the mission. In some entries the frequencies are underlined since they are a special extension of the low band into the high frequency range. These measurements have the property of a narrow 1 kHz bandwidth, but the sensitivity of the low band receivers falls off rapidly between 2.0 and 2.5 MHz. Similarly, it is possible to extend the high band receiver beyond its normal frequency range. For example, an in-flight receiver polarization test was performed at 47 MHz.

In some instances a second set of three FIXLO frequencies have been sampled in the same mode mixture with the regular FIXLO frames. These alternate FIXLO scans are designated FIXLO' in Tables 2 and 3 and the frequencies used are listed under F_4 , F_5 , and F_6 in Table 2. A frame of FIXLO' data has a different pattern of frequency measurement which is $F_6 F_4 F_5 F_4 F_6 F_4 F_5 F_4$. As shown in Table 3, FIXLO' was only used when Table indices 3, 6, 10 and 11 were in effect.

The PHIEX or POLHI "express" mode is a special extension of the POLHI mode which is designed for high time resolution, fixed-frequency studies. This mode can only be used when the spacecraft is in the GS2 imaging configuration. When the mode is executed, data can be returned at a rate of 14.4 K words per second, since the radio data are merged with the high-rate imaging data stream. Two frequencies can be chosen for study and these are listed in Table 2. Sampling of the two frequencies alternates in 24-second intervals. During the 24 seconds the readout of the measurements occurs every 69.4 microseconds alternating between the upper and lower channels and the left and right polarizations. Thus, in high band, two adjacent frequencies are being monitored, left-hand polarization from one and right-hand from the other. For low band the polarization alternates but the frequency remains the same throughout the 24-second interval.

Measurements are made in both channels simultaneously so that the integration time is 0.1 msec. Since no mode status words are contained in this data stream, the instrument status must be obtained from the POLHI data which are output in the normal PRA data stream at the same time.

Normal POLHI data scans consist of 2 mode status words followed by 198 data words taken at the same rate and in the same manner as for the PHIEX mode. Thus, useful data is taken for only 13.7 msec out of the 6 second interval. Since the amount of PHIEX data was more than originally anticipated, POLHI was very seldom implemented after the first few months of the mission.

The HARAD mode is a swept-frequency mode that is the same as POLLO in the high band but is centered on the spacecraft power supply harmonic frequencies in low band. The intent was to measure any excitation of the local plasma by the power supply wave form. This effect was never observed so HARAD has fallen into disfavor.

LEVEL is a swept-frequency calibration mode using the attenuators and an internal noise diode. It has been used several times in the mission especially for four hours before and after each encounter. In all cases the measurements showed no changes in the instrument performance.

DATA DESCRIPTION

Table 2 lists the implementation of the operating modes described in the previous section as they occurred in the mission through 1979 as well as other significant events affecting the data. The times of these events are recorded to the second where possible, but in some cases this accuracy was not available and the seconds or minutes columns have been left blank. The table index is indicative of the mode mixture which was commanded at a particular time and it is explained in Table 3. The frequencies sampled in the FIXLO mode are listed under the columns marked F_1 , F_2 , and F_3 . The order in which these frequencies are scanned was discussed in the previous section. The alternate FIXLO mode, FIXLO', uses the frequencies marked F_4 , F_5 , and F_6 . This mode is only used, however, when the table index is 3, 6, 10 or 11 as shown in Table 3. The same columns listing the FIXLO' frequencies have been used for the POLHI frequencies (P_1 , P_2 , and P_3) since the two modes were never used simultaneously. The PHIEX frequencies are listed in the columns marked P_1 and P_2 under PHIEX. The table index and frequencies are left blank when they have not changed from the previous event.

Finally, the comments column of Table 2 gives a capsule description of the reason for each entry. In most cases the entries describe data rate or mode mixture changes. Several times, however, unforeseen resets of the instrument occurred, described as power up resets. Instrument resets would result in all 90 dB of commandable attenuation being in effect for short periods of time until the previous mode was reestablished. Usually, very little data was lost and, since this problem became more frequent later in the mission, not all of the resets have been listed. In some instances 15 dB of attenuation was inserted for short periods of time, and the sudden change in the Jovian signal intensity is apparent in the data. Use of the attenuators was found to be unnecessary except near encounter so that very little of the data includes a commanded attenuation.

The spacecraft turnaround times indicate when the Voyagers were reoriented such that the measured polarization sense of the radio source reverses. (Short-term spacecraft maneuvers are not counted as turnaround

TABLE 2
VOYAGER 1 EVENTS

No.	Date Day	Yr.	Time Hr. Min.	Sec.	Table Index*	Frequencies (MHz)						Comments		
						F ₁	F ₂	F ₃	F ₄ /P ₁	F ₅ /P ₂	F ₆ /P ₃	P ₁	P ₂	
Sept.	5	77	15	22	12	1	0.19	0.31	0.25	0.06	0.21	0.25	7.99	0.56
Sept.	8	77	13	15	00		0.21	0.31	0.25	0.06	0.21	0.25		0.19 MHz was bad channel
Sept.	13	77	18	9	57									Cruise 6
Nov.	8	77	13	24	59									High data rate
Dec.	12	77	23	20			0.21	0.25	0.31	21.8	7.99	0.56		
Mar.	14	78	21	15	2									More PLL0 scans
June	7	78	13	12	47									Cruise 3
June	22	78	18	25	35	3	<u>1.50</u>	<u>2.00</u>	<u>2.44</u>	1.71	2.23	2.78	26.1	1.53
June	30	78	19	0	49									Even PLL0/FIXLO
July	6	78	15	49	07	1								Cruise 6
Aug.	3	78	00	10	3									7.99 0.56 Power Up Reset Recovery

* The table index refers to the mode mixture in effect. It is interpreted in Table 3.

** Data rates and Cruise modes are listed in Table 4.

+ Underlined frequencies are special extensions of the normal low band receiver frequency ranges.

TABLE 2
VOYAGER 1 EVENTS

Mon.	Date Day	Yr.	Time Hr. Min.	Sec.	Table Index*	Frequencies (MHz)			PHIEX	Comments
						FIXLO F ₁	FIXLO' / POLHI F ₂	F ₃		
Oct.	23	78	20	37	8	3	1.54	1.54	1.54	1.00 1.19
Dec.	5	78	0	4	55					High data rate
Dec.	8	78				4				Near encounter test
Dec.	10	78								30 dB Attenuation In
Dec.	12	78								0 dB Attenuation In
Dec.	15	78				3				POLLO-FIXLO
Dec.	19	78	19	11		20	6			9/10 POLLO
Jan.	13	79	12	34	59					Power Up Reset
Jan.	13	79	19	3						Power Up Reset Recovery
Jan.	30	79	11	49	23					Encounter Mode Mix
Feb.	2	79	4	35	00					Pre-encounter calibration
Feb.	2	79	4	57	26					LEVEL In
Feb.	2	79	8	35	00					Phase Calibration
Feb.	2	79	12	35	00					Calibration Out
Feb.	23	79	21	36	6					9.52 26.1

TABLE 2
VOYAGER 1 EVENTS

Mon.	Date Day	Yr.	Time			Table Index*	Frequencies (MHz)			Comments
			Hr.	Min.	Sec.		F ₁	F ₂	F ₃	
Feb.	24	79	2	9	24	8				HARAD In
Feb.	26	79	0	11	48					15 dB Attenuation In
Mar.	8	79	19	58	20					15 dB Attenuation Out
Mar.	11	79	10	57	32	7				LEVEL In
Mar.	11	79	14	39	56					Phase Calibration
Mar.	11	79	18	39	56	8				Calibration Out
Mar.	20	79	21	45	32	9				0.10 0.12 FIXLO In
Apr.	6	79	03	06	00					Spacecraft turnaround
Apr.	13	79	13	1	32	6				Cruise 4
July	28	79				4				A11 POLL0
Oct.	29	79	17	21	36	9				FIXLO In GS-3
Nov.	1	79	22	33	37	4				A11 POLL0
Nov.	20	79	17	21	37	9				FIXLO In GS-3
Nov.	22	79	00	10	00	4				A11 POLL0
Dec.	11	79	14	57	38	9				FIXLO In GS-3
Dec.	18	79				4				A11 POLL0

TABLE 2
VOYAGER 2 EVENTS

TABLE 2
VOYAGER 2 EVENTS

TABLE 2
VOYAGER 2 EVENTS

Table 3

Table Index Mode Mix Interpretation

<u>Table Index</u>	<u>Mode Mixture</u>
1	POLLO/LEVEL/HARAD/FIXLO/POLHI/POLLO/4 FIXLO/POLLO/ POLHI/3 FIXLO/POLLO/HARAD/3 FIXLO/POLLO/POLHI/3 FIXLO/ POLLO/2 FIXLO/POLHI/FIXLO
2	POLLO/LEVEL/HARAD/FIXLO/POLHI/FIXLO/5 POLLO/HARAD/ FIXLO/POLHI/FIXLO/5 POLLO/HARAD/FIXLO/POLHI/FIXLO/ POLHI/5 POLLO
3	POLLO/FIXLO/POLLO/FIXLO'/....
4	30 POLLO
5	29 FIXLO/POLLO
6	9 POLLO/FIXLO'/9 POLLO/FIXLO/9 POLLO/FIXLO'
7	LEVEL/29 POLLO
8	HARAD/29 POLLO
9	FIXLO/29 POLLO
10	FIXLO'/5 POLLO/FIXLO/5 POLLO/...
11	LEVEL/5 POLLO/FIXLO/5 POLLO/FIXLO'/5 POLLO/FIXLO/ 5 POLLO/FIXLO'/5 POLLO

times.) This occurs because the emission source is then on the opposite side of the antenna plane.

In the previous section we described the modes of operation and mentioned that these are usually grouped in frames consisting of a set of eight cycles of a particular mode. The time required to transmit a frame of data to the ground varies depending on the cruise mode of the spacecraft. These times are summarized in Table 4. In the highest data rate modes the frames are produced and transmitted continuously. The length of time to transmit a frame increases gradually with the other cruise modes except for Cruise-6. In Cruise-6 the data transmission rate is so low that the PRA frames are too widely separated in time to be generally useful. Consequently, for the times corresponding to Cruise-6 the data have not yet been processed. The times when each of the cruise modes were in effect and when data are available are shown in Figure 4. Note that Cruise-5 was not used through 1979, and Cruise-6 data are not shown since they are not available.

Figure 5 shows the flow of data after it has been transmitted by the spacecraft. Telemetry from the two Voyagers is routed to the Jet Propulsion Laboratories (JPL) where it is recorded. The data are then divided according to instrument and placed on Experimenter Data Record (EDR) tapes. The EDR tapes are not, however, in perfect time sequence. If JPL encounters any problems in a segment of the data the processing of that segment may be delayed and added to a later EDR tape. Delays in the receipt of data by JPL from the scattered tracking stations may also result in a jumbled time sequence. As a result, the EDR tapes often consist of blocks of synchronous data which are asynchronous with respect to each other. The same problems can also result in duplicate data appearing in the EDR tapes.

The PRA EDR tapes are then sent to the principle investigator, J. W. Warwick, at Radiophysics Inc., in Boulder, Colorado. The EDR data records are converted in a one-to-one ratio into Decalibrated Experimenter Data Records (DEDR) tapes by a translation of the measurements from telemetry counts into signal level at the receiver terminals expressed in millibels above a fixed lower voltage of $0.07 \cdot 10^{-6}$ V. (To convert from millibels to power flux

Table 4

Cruise Mode Data Rates

<u>Cruise Mode</u>	<u>Frame Completion Time (sec.)</u>
High Data Rate (GS3, Cruise 1, Cruise 2)	48
Cruise 3	96
Cruise 4	192
Cruise 5	240
Cruise 6	2880

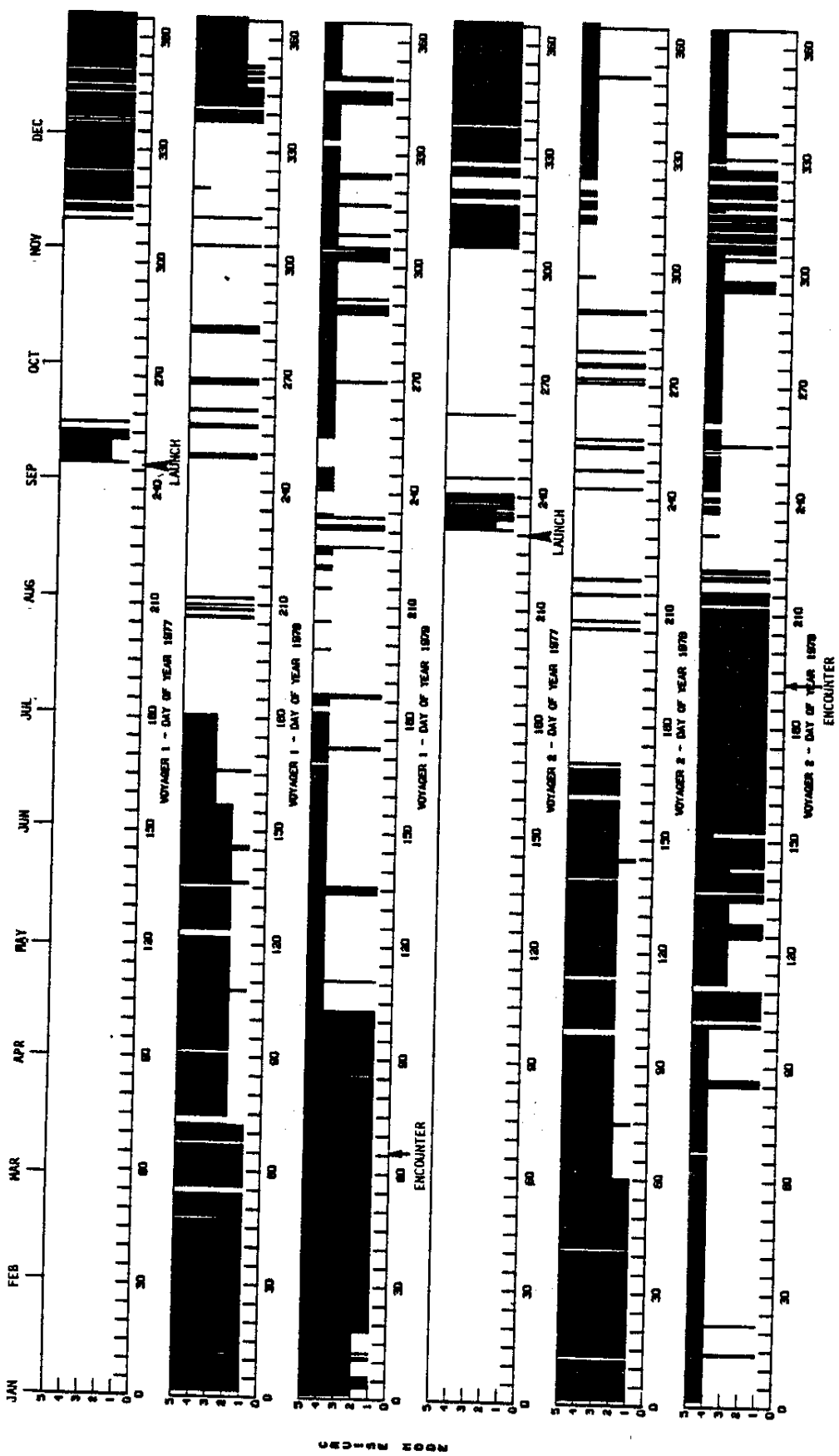


FIGURE 4. Plot of cruise mode versus time for each Voyager spacecraft. The black histogram bars extend downward from the lowest data rate, Cruise-5, to the Cruise mode in effect at the given time. The times when the GS2 and GS3 modes were in effect are grouped with Cruise 1. Cruise 5 was not used from launch through 1979. Cruise 6 times are not shown since these data are not available in the 48-second frame averages tapes.

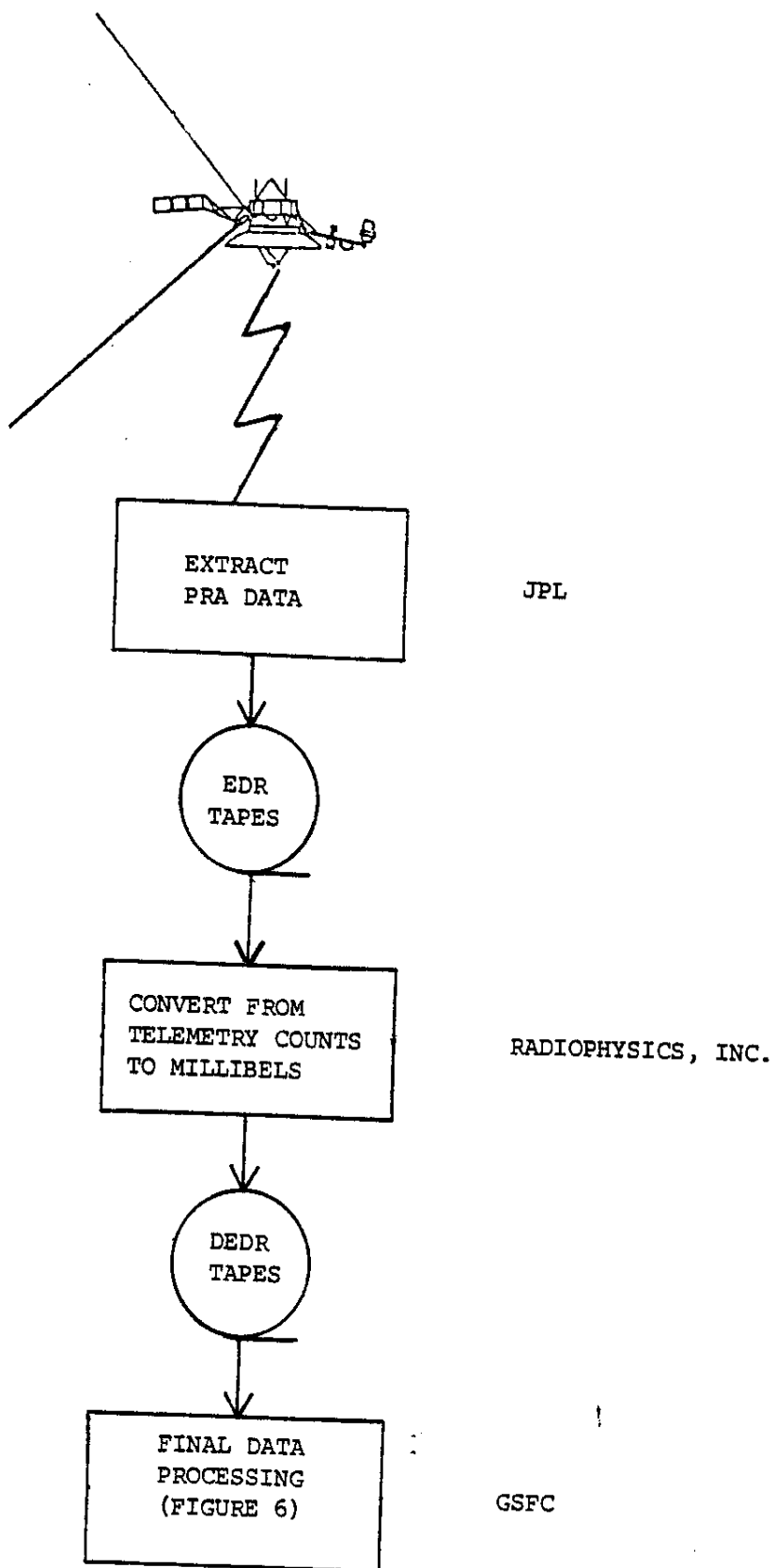


FIGURE 5. Flow of data from the spacecraft through initial processing and calibration at JPL and Radiophysics, Inc. to Goddard Space Flight Center.

densities at the antenna it should be assumed that zero millibels corresponds to $3.5 \times 10^{-22} \text{ W m}^{-2} \text{ Hz}^{-1}$ in each polarization channel.) The time order of the data remains the same.

Goddard Space Flight Center (GSFC) receives copies of the DEDR tapes from Radiophysics Inc. The flow of subsequent data processing is diagrammed in Figure 6. First, the DEDR tapes are copied, but the recording density is increased from 800 bits per inch to 6250 bits per inch in the process. The tape volume and times of coverage for these data are then recorded in a data catalog for possible future reference. At this point all of the POLLO frames are extracted from the data and a new tape is created based on averages of the signal for the eight scans in each frame. The result is the average signal for left and right polarizations within each frequency for the duration of the frame. The frame duration depends on the cruise mode in effect at the time, as shown in Table 4. After the frame-averaged data are sorted by time they are merged with the old master tape and any duplicate records are eliminated. The resultant master tape format is described in detail in Table 5.

Both DEDR and frame-averaged millibel tapes are stored at GSFC. For those interested in the data from modes other than the stepped-frequency POLLO mode, it will be necessary to begin with the DEDR tapes and search the status words of each record for the code representing the mode of interest. The processed POLLO data are directly available on eight tape volumes in the GSFC Systems and Applications Computing Center (SACC) tape library. The eight volumes and their dates of coverage are listed in Table 6. If the tapes are to be used with the SACC computers or if the user has access to a computer which has the Fortran Tape Input/Output (FTIO) system then the VTAPES subroutine can be used for direct mounting of the correct volume.

The bottom of Figure 6 demonstrates that the master tape of POLLO data serves as the starting point for the dynamic spectra plots. Through intermediate processing steps a plot tape suitable for the Versatec plotter is generated. This intermediate tape is used to generate the 24-hour plots described in the next section.

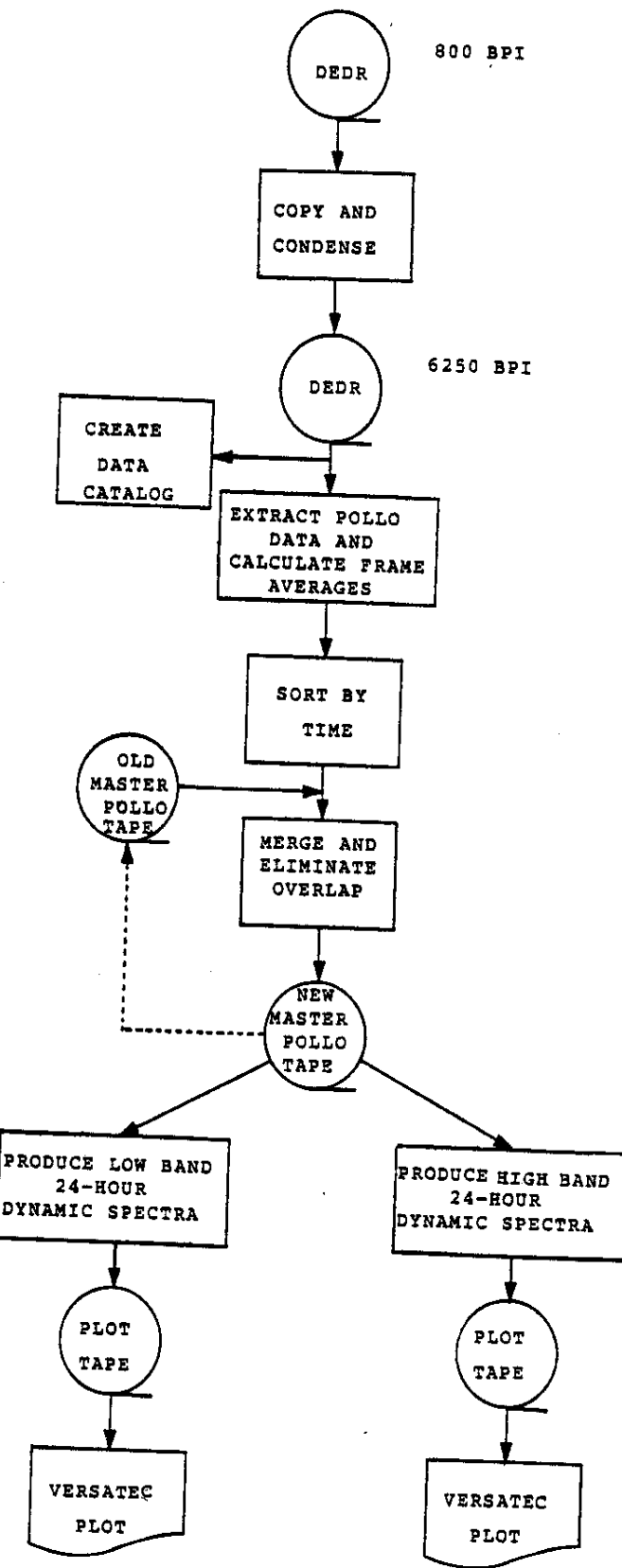


FIGURE 6. Flow of PRA data processing at Goddard Space Flight Center from receipt of the DEDR tapes from Radiophysics, Inc. to production of the dynamic spectra plots.

TABLE 5

VOYAGER FRAME AVERAGES TAPES

EACH LOGICAL RECORD CONTAINS THE AVERAGE VALUE IN MILLIBELS OF THE LH AND RH CHANNELS FOR EACH FREQUENCY FOR ONE VOYAGER POLLO FRAME (=8 SCANS, NOMINALLY 48 SECONDS). LOGICAL RECORDS ARE 808 8-BIT BYTES PLUS A 4 BYTE CONTROL WORD. PHYSICAL RECORDS ARE 32484 BYTES (40*812+4). DCB=(RECFM=VBS,LRECL=812, BLKSIZE=32484.....DENSITY=6250 BPI

THE FORMAT IS AS FOLLOWS:

WORD#	TYPE	BYTES	DESCRIPTION
1	I	4	DATE IN YYMMDD FORM, E.G. (MAY 24, 1978=780524)
2	I	4	SPACE-CRAFT EVENT TIME IN ELAPSED MILLISECONDS FROM 0 HOURS ON DATE(WORD 1), GIVEN AT THE START OF THE FRAME
3	I	4	TELEMETRY MODE...=7 OR 8(CR-1) =1(CR-2) =2(CR-3) =3(CR-4) =10(OS-3)
4-202	I	2	THE AVERAGED RECEIVED POWER FOR ALL 199(*) FREQUENCIES IN DESCENDING ORDER OVER THE FRAME IN MILLIBELS FOR LH AND RH CHANNELS

THE TAPE CAN BE READ AS FOLLOWS:

```

INTEGER*4 A(202)
INTEGER*2 AVE(199,2)      (*)
EQUIVALENCE (A(1),IYMD),(A(2),MSEC),(A(3),MODE),(A(4),AVE(1))
READ(IUNIT) A

```

- * NOTE THAT AVE IS DIMENSIONED 199 INSTEAD OF 198. THIS ALLOWS FOR THE 'EXTRA' FREQUENCY CHANNEL AVAILABLE IN HIGH BAND. POSITION 1 THUS CORRESPONDS TO 40550 KHZ (AND IS USUALLY ALL ZEROS). POSITION 129 CORRESPONDS TO 1228.8 KHZ. LOW BAND IS CONTAINED IN POSITIONS 130 TO 199. ALSO, LH AVERAGES ARE STORED IN AVE(I,1), AND RH AVERAGES ARE STORED IN AVE(I,2).

TABLE 6
MILLIBEL TAPE VOLUMES

The following tapes are in the tape library in the building 1 Systems and Applications Computing Center (SACC) at Goddard Space Flight Center. The format of the tapes is described in Table 5. Copies or direct use of these tapes can be arranged through J. K. Alexander or M. L. Kaiser, Laboratory for Extraterrestrial Physics, Code 695, Goddard Space Flight Center, Greenbelt, Maryland 20771.

<u>TAPE VOLUME</u>	<u>DATA SET NAME</u>	<u>DATES OF COVERAGE</u>
RA0001	VOYAGER1.AVG	Sept. 5, 77-June 30, 78
RA0002	VOYAGER1.AVG	July 1, 78-Feb. 28, 79
RA0003	VOYAGER1.AVG	March 1, 79-July 31, 79
RA0004	VOYAGER1.AVG	Aug. 1, 79-Dec. 31, 79
RA0010	VOYAGER2.AVG	Aug. 20, 77-June 30, 78
RA0011	VOYAGER2.AVG	July 1, 78-May 31, 79
RA0012	VOYAGER2.AVG	June 1, 79-Aug. 10, 79
RA0013	VOYAGER2.AVG	Aug. 19, 79-Dec. 31, 79

VTAPES Subroutines

A Fortran subroutine, written by P. G. Harper, is available on the SACC computer which will automatically mount the correct millibel tape given the spacecraft, the time period, and the Fortran input device unit number. This requires the use of the Fortran Tape Input/Output (FTIO) system. Thus, the data must be read in with an FREAD statement as described in the FTIO manual. The CALL statement is as follows:

CALL VTAPES (ID, ITYPE, IYMD, IUNIT)

where all four arguments are integers and

ID = 1 or 2 for Voyager 1 or 2

ITYPE = 1 for millibel tapes

IYMD = YYMMDD, six digit integer giving the year, month, and day for the data required

IUNIT = Fortran input device number corresponding to XX in the data definition card below

The IBM data definition card appears below. XX is to chosen by the user.

```
//FTXXF001 DD UNIT=(6250,,DEFER),LABEL=(,SL),DCB=RECFM=VBS
```

The subroutine is found in the library with data set name M2.U3MLK.LODMOD. Note that the subroutine need only be called with the starting date for a span of many days of data, unless the dates extend beyond the end of a tape. Consecutive calls to VTAPES will result in a tape mount request only if a new tape is required.

DYNAMIC SPECTRA PLOTS

The POLLO data have been used to generate 24-hour dynamic spectra plots. Copies of these plots extending through the end of 1979 have been stored at the NSSDC with this document. The plots are divided into high band and low band, and Figures 7, 8, and 9 are examples of these. Since the high band is considerably lower in sensitivity than low band, meaningful high frequency data were only obtained within several months of Jupiter encounters. Consequently, the stored high band records do not span the full range of time from launch to December 31, 1979, but only from Feb. 1, 1979 to Apr. 29, 1979 for Voyager 1 and May 1, 1979 to Aug. 10, 1979 for Voyager 2.

The plots exemplified by Figures 7 and 8 are produced on a 12 inch Versatec electrostatic plotter with 200 dot/inch resolution. In their original form, the only explanatory markings which appear are the large block letters on the right side of each plot. Extra annotation has been added to each figure to explain the tic marks along the axes and the meanings of the block letters. In each case the plots are composed of four panels. The vertical axis represents the high or low band frequency scale. Note that frequency increases in the downward direction. The horizontal axis represents spacecraft event time. In the lower three panels the darkness is proportional to the logarithmic intensity of the signal above a computed background. The background is calculated for each frequency in each consecutive group of 500 frame averages. It represents an iterative average of the signal level calculated after excluding the highest and lowest signals until the standard deviation is within a predetermined value. Such a variable background was found necessary so that the plot can display differences in signal strength for both weak emission far from Jupiter and the strong emission during encounter. The lower two panels represent the frame averages of right and left hand polarization measurements and the sum of these two is shown in the total power panel. Their difference gives the polarization sense displayed in the top panel, where white (black) represents a dominance of right hand (left hand) polarization.

July 4, 1979

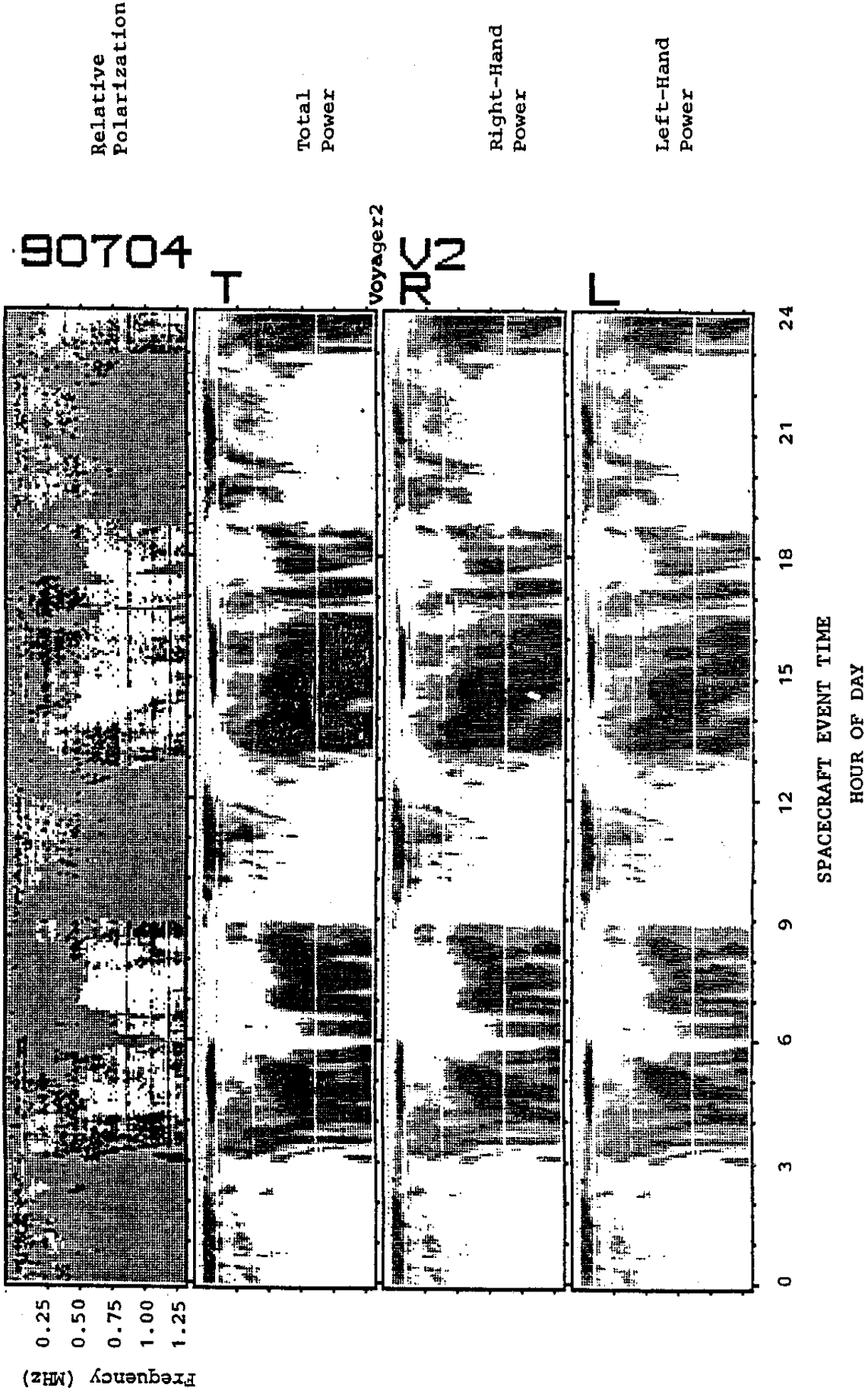


FIGURE 7. Example of 24-hour low-band dynamic spectra plot data received by Voyager 2 on July 4, 1979. The lower three panels are shaded in proportion to the logarithm of the signal strength for left-hand, right-hand, and total power (sum of left and right). The top panel is shaded in accordance with polarization, from white for right-hand dominance to black for left-hand dominance.

790704

T

K2

L

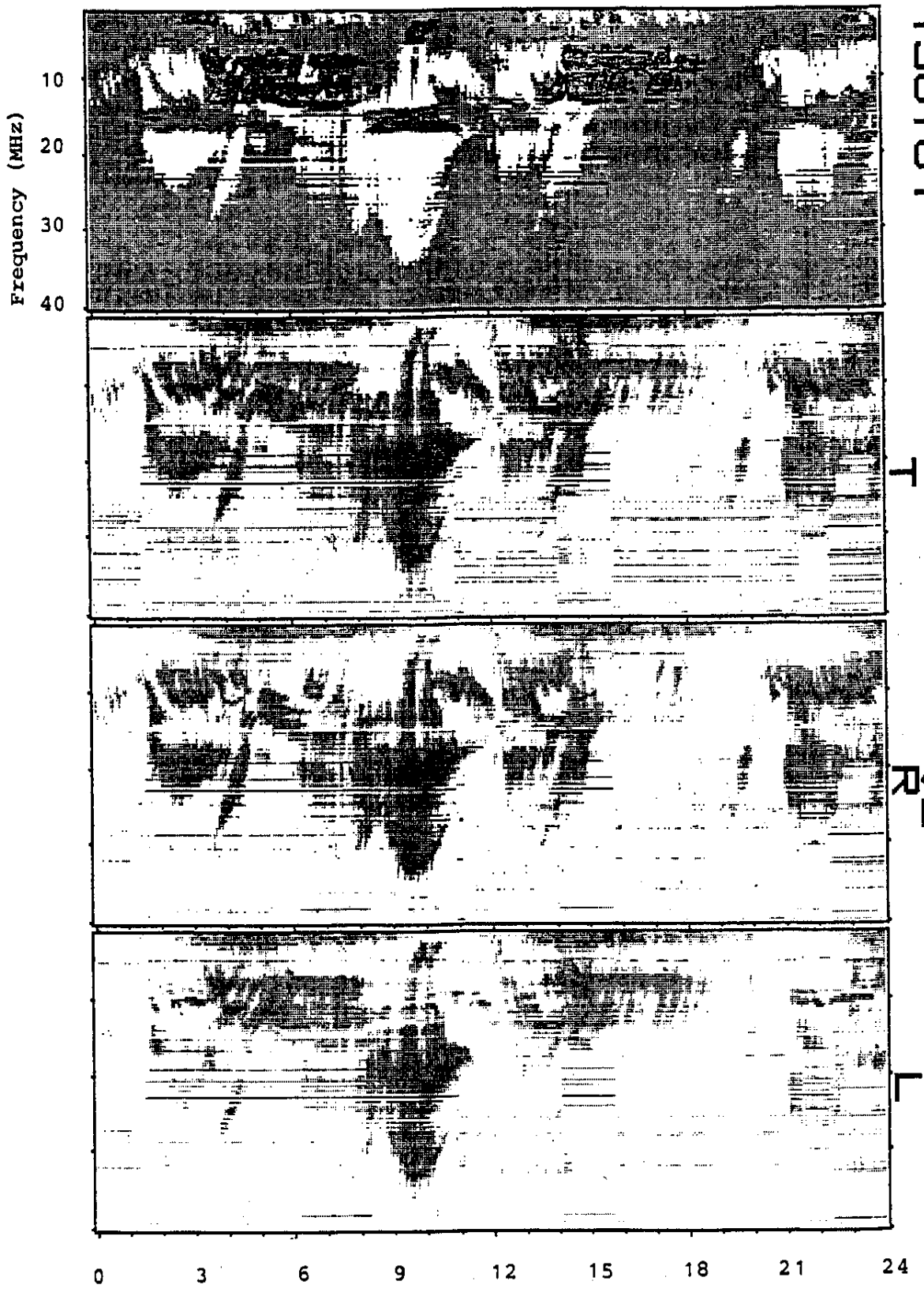


FIGURE 8. Same as Figure 7 except for high band frequencies.

790709

T

R2

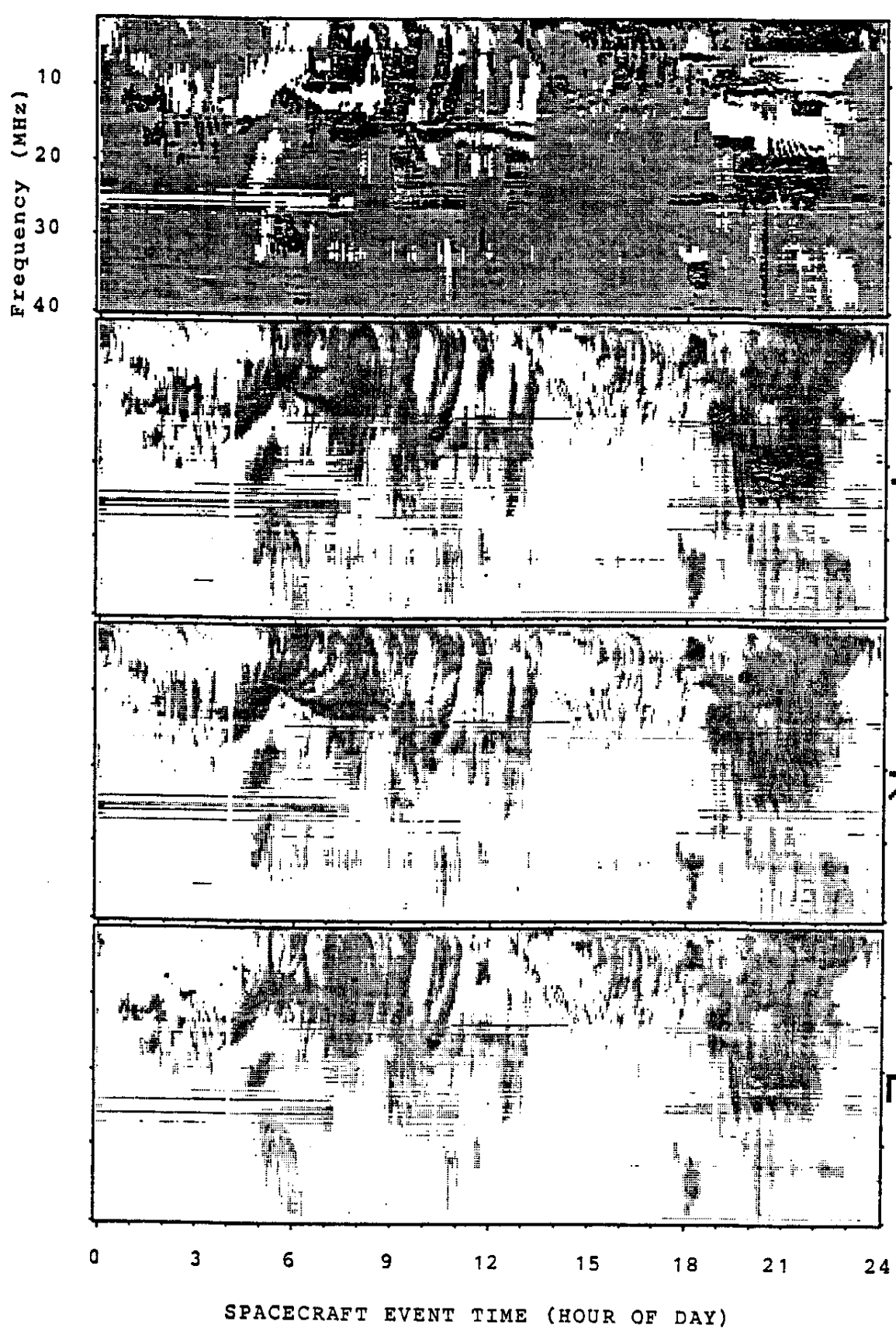


FIGURE 9. Same as Figure 8 except for data from July 9, 1979. The figure illustrates high-frequency (greater than 25 MHz) "ghost mirror images appearing as a result of strong lower frequency (less than 10 MHz) signals. The images are elongated in frequency span. The appearance at 18 hours is a good example.

All 70 channels are displayed in the low band plot. The presence of the horizontal streaks shows the problem of spacecraft interference which made some of the channels permanently unusable. Of the 129 possible channels in high band, 128 are displayed. The lowest frequency, 1.2 MHz, is not shown since it overlaps the low band frequencies. As discussed earlier the highest frequency, 40.5 MHz, is never sampled in the lower channel POLLO sampling mode so it is always zero. Interpretation of these and similar plots has been discussed in many of the references listed in the bibliography.

PRA PUBLICATIONS

This section summarizes the research which has been published based on the PRA data described in this document. We have already referred to the pre-launch publications by Warwick et al. (1977) and Lang and Peltzer (1977) describing the instrument. The initial observations using the PRA instrument were concentrated on Terrestrial Kilometric Radiation (TKR). A paper describing these observations was published by Kaiser et al. (1978) who presented the first direct polarization measurements of TKR and confirmed that the emission is generated in the extraordinary mode.

Very soon after leaving the earth the PRA instrument began to detect Jovian radio emissions in low band. These initial observations at hectometric (HOM) wavelengths are described in Kaiser et al (1979). An explanation of the longitudinal profile of these emissions was put forth in Alexander et al. (1979). A more recent discussion of the dynamic spectra of the HOM component of the emission is given by Lecacheux et al. (1980).

The encounters of Voyagers 1 and 2 with Jupiter resulted in a large variety of new information. Overviews reflecting on the initial results were published in special issues of Science (Warwick et al., 1979a and 1979b). Since the encounters there has been time to study the many phenomena in more detail. Most of these results will appear in a special issue of the Journal of Geophysical Research to be published in the spring of 1981. An overview paper (Boischt et al., 1981) will be published in that issue which describes much of the work to date.

Research on the PRA data has been concentrated in several areas. The newly-discovered Jovian Kilometric Radiation (JKR or KOM) has been analyzed by Kaiser and Desch (1980) and Desch and Kaiser (1980). Alexander et al. (1981) described the general statistical properties of both the high band-and low-band observations, especially in their relationship to previous ground-based results. Many groups have become interested in the study of the arc-like patterns which appear in the dynamic spectral plots of high-band data taken close to encounter. The publications on this topic are by Boischot and Aubier (1981), Goldstein and Thieman (1981), Leblanc (1981), Pearce (1981), Staelin (1981), and Warwick (1981).

During the Voyager 1 Jupiter encounter the spacecraft traveled through the Io plasma torus and made direct measurements of the electron plasma frequency. Birmingham et al. (1981) used these measurements as a basis for modelling the plasma structure within the plasma torus. Lecacheux (1981) performed ray tracing calculations to consider the effects of the torus on the Jovian radio emission measured during the encounter.

Other topics of interest are currently under investigation and further inquiries on the work in progress should be directed to the investigators listed in the above publications.

ACKNOWLEDGMENTS

We wish to thank J. K. Alexander, M. L. Kaiser, J. B. Pearce, and P. G. Harper who have cheerfully undergone considerable interrogation in the course of the preparation of this document. We are also grateful for their provision of much of the material used directly or indirectly in the tables. This document was prepared in accordance with NASA contract number NAS5-25932.

PRA BIBLIOGRAPHY

- Alexander, J. K., M.D. Desch, M. L. Kaiser, and J. R. Thieman, Latitudinal beaming of Jupiter's low frequency radio emission, J. Geophys. Res., 84, 5167, 1979.
- Alexander, J. K., T. D. Carr, J. R. Thieman, J. J. Schauble and A. C. Riddle, Synoptic observation of Jupiter's radio emissions: average statistical properties observed by Voyager, J. Geophys. Res., in press, 1981.
- Birmingham, T. J., J. K. Alexander, M. D. Desch, R. F. Hubbard and B. M. Pedersen, Observations of electron gyroharmonic waves and the structure of the Io plasma torus, J. Geophys. Res., in press, 1981.
- Boisshot, A., and M. Aubier, The Jovian decametric arcs as an interference pattern, J. Geophys. Res., in press, 1981.
- Boisshot, A., A. Lecacheux, M. L. Kaiser, M. D. Desch, J. K. Alexander and J. W. Warwick, Radio Jupiter after Voyager: an overview of the planetary radio astronomy observations, J. Geophys. Res., in press, 1981.
- Desch, M. D. and M. L. Kaiser, The occurrence rate, polarization character, and intensity of broadband Jovian kilometric radiation, J. Geophys. Res., 85, 4248, 1980.
- Goldstein, M. L. and J. R. Thieman, On the formation of arcs in the dynamic spectra of Jovian decameter bursts, J. Geophys. Res., in press, 1981.
- Kaiser, M. L., J. K. Alexander, A.C. Riddle, J. B. Pearce and J. W. Warwick, Direct measurement by Voyagers 1 and 2 of the polarization of terrestrial Kilometric radiation, Geophys. Res. Lett., 5, 857, 1978.
- Kaiser, M. L., M. D. Desch, A. C. Riddle, A. Lecacheux, J. B. Pearce, J. K. Alexander, J. W. Warwick, and J. R. Thieman, Voyager spacecraft radio observations of Jupiter: initial cruise results, Geophys. Res. Lett., 6, 507, 1979.

Kaiser, M. L. and M. D. Desch, Narrow band Jovian kilometric emission: a new radio component, Geophys. Res. Lett., 7, 389, 1980.

Lang, G. J., and R. G. Peltzer, Planetary radio astronomy receiver, IEEE Trans., AES13, 466, 1977.

Leblanc, Y., On the arc structure of the DAM Jovian emission, J. Geophys. Res., in press, 1981.

Lecacheux, A., Ray tracing in the Io plasma torus; application to the PRA observations during Voyager 1's closest approach, J. Geophys. Res., in press, 1981.

Lecacheux, A., B. Pedersen, A. C. Riddle, J. B. Pearce, A. Boischot and J. W. Warwick, Some spectral characteristics of the hectometric Jovian emission, J. Geophys. Res., in press, 1980.

Pearce, J. B., A heuristic model for the Jovian decametric arcs, J. Geophys. Res., in press, 1981.

Staelin, D. H., Character of the Jovian decametric arcs, J. Geophys. Res., in press, 1981.

Warwick, J. W. Models for decametric arcs, J. Geophys. Res., in press, 1981.

Warwick, J. W., J. B. Pearce, R. G. Peltzer, and A. C. Riddle, Planetary radio astronomy experiment for the Voyager missions, Space Sci. Rev., 21, 309, 1977.

Warwick, J. W., J. B. Pearce, A. C. Riddle, J. K. Alexander, M. D. Desch, M. L. Kaiser, J. R. Thieman, T. D. Carr, S. Gulkis, A. Boischot, C. C. Harvey, and B. M. Pedersen, Voyager 1 planetary radio astronomy observations near Jupiter, Science, 204, 955, 1979a.

Warwick, J. W., J. B. Pearce, A. C. Riddle, J. K. Alexander, M. D. Desch, M. L. Kaiser, J. R. Thieman, T. D. Carr, S. Gulkis, A. Boischot, Y. LeBlanc, B. M. Pedersen, and D. H. Staelin, Planetary radio astronomy observations from Voyager 2 near Jupiter, Science, 206, 991, 1979b.

Table A-1
Voyager 2 Antenna Angles
seen normal to antenna plane and Jupiter

Table A-1 (cont.)
Voyager 2 Antenna Angles

θ = Angle between normal to antenna plane and Jupiter

Yr/Mo/Day	Hr/Min/Sec	θ	Yr/Mo/Day	Hr/Min/Sec	θ	Yr/Mo/Day	Hr/Min/Sec	θ
79C7C4	185	247	79C7C4	67	7	79C7C4	101	6
79C7C4	186	247	79C7C4	68	7	79C7C4	102	7
79C7C4	187	247	79C7C4	69	7	79C7C4	103	8
79C7C4	188	247	79C7C4	70	7	79C7C4	104	9
79C7C4	189	247	79C7C4	71	7	79C7C4	105	10
79C7C4	190	247	79C7C4	72	7	79C7C4	106	11
79C7C4	191	247	79C7C4	73	7	79C7C4	107	12
79C7C4	192	247	79C7C4	74	7	79C7C4	108	13
79C7C4	193	247	79C7C4	75	7	79C7C4	109	14
79C7C4	194	247	79C7C4	76	7	79C7C4	110	15
79C7C4	195	247	79C7C4	77	7	79C7C4	111	16
79C7C4	196	247	79C7C4	78	7	79C7C4	112	17
79C7C4	197	247	79C7C4	79	7	79C7C4	113	18
79C7C4	198	247	79C7C4	80	7	79C7C4	114	19
79C7C4	199	247	79C7C4	81	7	79C7C4	115	20
79C7C4	200	247	79C7C4	82	7	79C7C4	116	21
79C7C4	201	247	79C7C4	83	7	79C7C4	117	22
79C7C4	202	247	79C7C4	84	7	79C7C4	118	23
79C7C4	203	247	79C7C4	85	7	79C7C4	119	24
79C7C4	204	247	79C7C4	86	7	79C7C4	120	25
79C7C4	205	247	79C7C4	87	7	79C7C4	121	26
79C7C4	206	247	79C7C4	88	7	79C7C4	122	27
79C7C4	207	247	79C7C4	89	7	79C7C4	123	28
79C7C4	208	247	79C7C4	90	7	79C7C4	124	29
79C7C4	209	247	79C7C4	91	7	79C7C4	125	30
79C7C4	210	247	79C7C4	92	7	79C7C4	126	31
79C7C4	211	247	79C7C4	93	7	79C7C4	127	32
79C7C4	212	247	79C7C4	94	7	79C7C4	128	33
79C7C4	213	247	79C7C4	95	7	79C7C4	129	34
79C7C4	214	247	79C7C4	96	7	79C7C4	130	35
79C7C4	215	247	79C7C4	97	7	79C7C4	131	36
79C7C4	216	247	79C7C4	98	7	79C7C4	132	37
79C7C4	217	247	79C7C4	99	7	79C7C4	133	38
79C7C4	218	247	79C7C4	100	7	79C7C4	134	39
79C7C4	219	247	79C7C4	101	7	79C7C4	135	40
79C7C4	220	247	79C7C4	102	7	79C7C4	136	41
79C7C4	221	247	79C7C4	103	7	79C7C4	137	42
79C7C4	222	247	79C7C4	104	7	79C7C4	138	43
79C7C4	223	247	79C7C4	105	7	79C7C4	139	44
79C7C4	224	247	79C7C4	106	7	79C7C4	140	45
79C7C4	225	247	79C7C4	107	7	79C7C4	141	46
79C7C4	226	247	79C7C4	108	7	79C7C4	142	47
79C7C4	227	247	79C7C4	109	7	79C7C4	143	48
79C7C4	228	247	79C7C4	110	7	79C7C4	144	49
79C7C4	229	247	79C7C4	111	7	79C7C4	145	50
79C7C4	230	247	79C7C4	112	7	79C7C4	146	51
79C7C4	231	247	79C7C4	113	7	79C7C4	147	52
79C7C4	232	247	79C7C4	114	7	79C7C4	148	53
79C7C4	233	247	79C7C4	115	7	79C7C4	149	54
79C7C4	234	247	79C7C4	116	7	79C7C4	150	55
79C7C4	235	247	79C7C4	117	7	79C7C4	151	56
79C7C4	236	247	79C7C4	118	7	79C7C4	152	57
79C7C4	237	247	79C7C4	119	7	79C7C4	153	58
79C7C4	238	247	79C7C4	120	7	79C7C4	154	59
79C7C4	239	247	79C7C4	121	7	79C7C4	155	60
79C7C4	240	247	79C7C4	122	7	79C7C4	156	61
79C7C4	241	247	79C7C4	123	7	79C7C4	157	62
79C7C4	242	247	79C7C4	124	7	79C7C4	158	63
79C7C4	243	247	79C7C4	125	7	79C7C4	159	64
79C7C4	244	247	79C7C4	126	7	79C7C4	160	65
79C7C4	245	247	79C7C4	127	7	79C7C4	161	66
79C7C4	246	247	79C7C4	128	7	79C7C4	162	67
79C7C4	247	247	79C7C4	129	7	79C7C4	163	68
79C7C4	248	247	79C7C4	130	7	79C7C4	164	69
79C7C4	249	247	79C7C4	131	7	79C7C4	165	70
79C7C4	250	247	79C7C4	132	7	79C7C4	166	71
79C7C4	251	247	79C7C4	133	7	79C7C4	167	72
79C7C4	252	247	79C7C4	134	7	79C7C4	168	73
79C7C4	253	247	79C7C4	135	7	79C7C4	169	74
79C7C4	254	247	79C7C4	136	7	79C7C4	170	75
79C7C4	255	247	79C7C4	137	7	79C7C4	171	76
79C7C4	256	247	79C7C4	138	7	79C7C4	172	77
79C7C4	257	247	79C7C4	139	7	79C7C4	173	78
79C7C4	258	247	79C7C4	140	7	79C7C4	174	79
79C7C4	259	247	79C7C4	141	7	79C7C4	175	80
79C7C4	260	247	79C7C4	142	7	79C7C4	176	81
79C7C4	261	247	79C7C4	143	7	79C7C4	177	82
79C7C4	262	247	79C7C4	144	7	79C7C4	178	83
79C7C4	263	247	79C7C4	145	7	79C7C4	179	84
79C7C4	264	247	79C7C4	146	7	79C7C4	180	85
79C7C4	265	247	79C7C4	147	7	79C7C4	181	86
79C7C4	266	247	79C7C4	148	7	79C7C4	182	87
79C7C4	267	247	79C7C4	149	7	79C7C4	183	88
79C7C4	268	247	79C7C4	150	7	79C7C4	184	89
79C7C4	269	247	79C7C4	151	7	79C7C4	185	90
79C7C4	270	247	79C7C4	152	7	79C7C4	186	91
79C7C4	271	247	79C7C4	153	7	79C7C4	187	92
79C7C4	272	247	79C7C4	154	7	79C7C4	188	93
79C7C4	273	247	79C7C4	155	7	79C7C4	189	94
79C7C4	274	247	79C7C4	156	7	79C7C4	190	95
79C7C4	275	247	79C7C4	157	7	79C7C4	191	96
79C7C4	276	247	79C7C4	158	7	79C7C4	192	97
79C7C4	277	247	79C7C4	159	7	79C7C4	193	98
79C7C4	278	247	79C7C4	160	7	79C7C4	194	99
79C7C4	279	247	79C7C4	161	7	79C7C4	195	00
79C7C4	280	247	79C7C4	162	7	79C7C4	196	01
79C7C4	281	247	79C7C4	163	7	79C7C4	197	02
79C7C4	282	247	79C7C4	164	7	79C7C4	198	03
79C7C4	283	247	79C7C4	165	7	79C7C4	199	04
79C7C4	284	247	79C7C4	166	7	79C7C4	200	05
79C7C4	285	247	79C7C4	167	7	79C7C4	201	06
79C7C4	286	247	79C7C4	168	7	79C7C4	202	07
79C7C4	287	247	79C7C4	169	7	79C7C4	203	08
79C7C4	288	247	79C7C4	170	7	79C7C4	204	09
79C7C4	289	247	79C7C4	171	7	79C7C4	205	10
79C7C4	290	247	79C7C4	172	7	79C7C4	206	11
79C7C4	291	247	79C7C4	173	7	79C7C4	207	12
79C7C4	292	247	79C7C4	174	7	79C7C4	208	13
79C7C4	293	247	79C7C4	175	7	79C7C4	209	14
79C7C4	294	247	79C7C4	176	7	79C7C4	210	15
79C7C4	295	247	79C7C4	177	7	79C7C4	211	16
79C7C4	296	247	79C7C4	178	7	79C7C4	212	17
79C7C4	297	247	79C7C4	179	7	79C7C4	213	18
79C7C4	298	247	79C7C4	180	7	79C7C4	214	19
79C7C4	299	247	79C7C4	181	7	79C7C4	215	20
79C7C4	300	247	79C7C4	182	7	79C7C4	216	21
79C7C4	301	247	79C7C4	183	7	79C7C4	217	22
79C7C4	302	247	79C7C4	184	7	79C7C4	218	23
79C7C4	303	247	79C7C4	185	7	79C7C4	219	24
79C7C4	304	247	79C7C4	186	7	79C7C4	220	25
79C7C4	305	247	79C7C4	187	7	79C7C4	221	26
79C7C4	306	247	79C7C4	188	7	79C7C4	222	27
79C7C4	307	247	79C7C4	189	7	79C7C4	223	28
79C7C4	308	247	79C7C4	190	7	79C7C4	224	29
79C7C4	309	247	79C7C4	191	7	79C7C4	225	30
79C7C4	310	247	79C7C4	192	7	79C7C4	226	31
79C7C4	311	247	79C7C4	193	7	79C7C4	227	32
79C7C4	312	247	79C7C4	194	7	79C7C4	228	33
79C7C4	313	247	79C7C4	195	7	79C7C4	229	34
79C7C4	314	247	79C7C4	196	7	79C7C4	230	35
79C7C4	315	247	79C7C4	19				

Table A-1 (cont.)
 Voyager 1 Antenna Angles
 θ = Angle between normal to antenna plane and Jupiter

Table A-1 (Cont.)
 Voyager Antenna Angles
 θ = Angle between normal to antenna plane and Jupiter

Table A-1 (Cont.)
 Voyager Antenna Angles
 θ = Angle between normal to antenna plane and Jupiter

Yr/Mo/Day	Hr/Min/Sec	θ
790015	212356	57.3
790016	212344	56.3
790016	142008	57.3
790016	141508	58.3
790016	141556	59.3
790017	141556	58.3
790017	141508	57.3
790017	182008	56.2
790018	102006	57.2
790018	142006	58.3
790019	172006	57.2
790019	121500	56.1
790020	112126	57.2
790021	630006	57.2
790022	171244	57.1
790022	102444	56.1
790022	1600044	57.1
790027	1000044	56.1
790028	2000044	57.1
790029	1000044	56.1
790030	112244	57.1
790031	104444	57.2
790031	201644	56.1
790031	194444	57.2
790032	1600044	56.2
790032	112244	57.2
790034	111244	56.2
790035	174444	57.2
790036	112444	56.5
790039	4844	132.5
790409	180044	133.5
791206	150049	45.7
		46.7

TABLE A-2

PRA RECEIVER FREQUENCIES

Ch. #	Freq. (KHz)	Ch. #	Freq. (KHz)
1	40550.2	29	31948.6
2	40243.0	30	31641.4
3	39935.8	31	31334.2
4	39628.6	32	31027.0
5	39321.4	33	30719.8
6	39014.2	34	30412.6
7	38707.0	35	30105.4
8	38399.8	36	29798.2
9	38092.6	37	29491.0
10	37785.4	38	29183.8
11	37478.2	39	28876.6
12	37171.0	40	28569.4
13	36863.8	41	28282.2
14	36556.6	42	27955.0
15	36249.4	43	27647.8
16	35942.2	44	27340.6
17	35635.0	45	27033.4
18	35327.8	46	26726.2
19	35020.6	47	26419.0
20	34713.4	48	26111.8
21	34406.2	49	25804.6
22	34099.0	50	25497.4
23	33791.8	51	25190.2
24	33484.6	52	24883.0
25	33177.4	53	24575.8
26	32870.2	54	24268.6
27	32563.0	55	23981.4
28	32255.8	56	23654.2

TABLE A-2 (Cont.)

PRA RECEIVER FREQUENCIES (Cont.)

Ch. #	Freq. (KHz)	Ch. #	Freq. (KHz)
57	23347.0	87	14131.0
58	23039.8	88	13823.8
59	22732.6	89	13516.6
60	22425.4	90	13209.4
61	22118.2	91	12902.2
62	21811.0	92	12595.0
63	21503.8	93	12287.8
64	21196.6	94	11980.6
65	20889.4	95	11673.4
66	20582.2	96	11366.2
67	20275.0	97	11059.0
68	19967.8	98	10751.8
69	19660.6	99	10444.6
70	19353.4	100	10137.4
71	19046.2	101	9830.2
72	18739.0	102	9523.0
73	18431.8	103	9215.8
74	18124.6	104	8908.6
75	17817.4	105	8601.4
76	17510.2	106	8294.2
77	17203.0	107	7987.0
78	16895.8	108	7679.8
79	16588.6	109	7372.6
80	16281.4	110	7065.4
81	15974.2	111	6758.2
82	15667.0	112	6451.0
83	15359.8	113	6143.8
84	15052.6	114	5836.6
85	14745.4	115	5529.4
86	14438.2	116	5222.2

TABLE A-2 (Cont.)

PRA RECEIVER FREQUENCIES (Cont.)

Ch. #	Freq. (KHz)	Ch. #	Freq. (KHz)
117	4915.0	147	980.4
118	4607.8	148	961.2
119	4300.6	149	942.0
120	3993.4	150	922.8
121	3686.2	151	903.6
122	3379.0	152	884.4
123	3071.8	153	865.2
124	2764.6	154	846.0
125	2457.4	155	826.8
126	2150.2	156	807.6
127	1843.0	157	788.4
128	1535.8	158	769.2
129	1326.0	159	750.0
130	1306.8	160	730.8
131	1287.6	161	711.6
132	1268.4	162	692.4
133	1249.2	163	673.2
134	1230.0	164	654.0
135	1210.8	165	634.8
136	1191.6	166	615.6
137	1172.4	167	596.4
138	1153.2	168	577.2
139	1134.0	169	558.0
140	1114.8	170	538.8
141	1095.6	171	519.6
142	1076.4	172	500.4
143	1057.2	173	481.2
144	1038.0	174	462.0
145	1018.8	175	442.8
146	999.6	176	423.6

TABLE A-2 (Cont.)

PRA RECEIVER FREQUENCIES (Cont.)

Ch. #	Freq. (KHz)	Ch. #	Freq. (KHz)
177	404.4		
178	385.2		
179	366.0		
180	346.8		
181	327.6		
182	308.4		
183	289.2		
184	270.0		
185	250.8		
186	231.6		
187	212.4		
188	193.2		
189	174.0		
190	154.8		
191	135.6		
192	116.4		
193	97.2		
194	78.0		
195	58.8		
196	39.6		
197	20.4		
198	1.2		

```

2 - SUBCHARGE=TOPIVES ALLOC=NO*TAPEMOUNTS=NO*CORE=000*PAPER=000*PRORITY=000001SECs
3   XG0  EXEC PGME=LINK,SYSLMOD COND=(4,1) REGION=70K
4   XFT05F001 DD DNAME=DATAS
5   XFT05F001 DD SYSDUT=80T,DCB=(RECFM=VBA,LRECL=137,BLKSIZE=6,BLKSIZE=1)
6   IEF6531 SUBSTITUTION JCL - SYSDUT=A,DCB=(RECFM=VBA,LRECL=137,BLKSIZE=72651)
7   XFT05F001 DD SYSDUT=B,DCB=(RECFM=FB,BLKSIZE=280,LRECL=80)
8   XSYSPRINT SUBSTITUTION JCL - SYSDUT=A,DCB=(RECFM=VBA,LRECL=137,BLKSIZE=1*0000300
9   IEF6531 SUBSTITUTION JCL - SYSDUT=A,DCB=(RECFM=VBA,LRECL=137,BLKSIZE=72651,
10   // SPACE=(CYL,0,5),UNIT=DISK,37,00000310
11   // VOL=SER=JJ0101
12   // GO,FTOBFO01 DD UNIT=6250,DISP=(OLD,KEEP),LABEL=(01,ELP..IN).
13   IEF2361 ALLC FOR YZRWPPBR6 GO
14   IEF2371 235 ATTACHED TO FT05F001
15   IEF2371 232 ALLOCATED TO FT06F001
16   IEF2371 237 ALLOCATED TO SYSPRINT
17   IEF2371 232 ALLOCATED TO SYSPRINT
18   IEF2371 235 ALLOCATED TO SYSDUMP
19   IEF2371 236 ALLOCATED TO SYSDUMP
20   IEF2371 490 ALLOCATED TO FT08F001

```

Vorpage 1

RECORD 2073 OF FILE 1									
1	2	3	4	5	6	7	8	9	10
1	0A290A41	0A290A4D	0A250RAA	0R680A1D	0AE20A4D	0B840A0D	0ASD0A6C	0F1CODE	0A2D0B1C
2	09FC0C12	0AF50A21	0A50D9DB	0CF30A25	0A970B1C	0E070BB4	0C3F0EAS	05F0000	09C00C4
3	0A060A46	0AC60R0E	0C0F0C43	0C600CD	106F0AA	0C570D42	0AF20BF2	0A010B07	080H0C02
4	08A540A43	0AE50A35	0A030RA	0ADBOATC	0ABCR0C0	0ASB0A4D	0A4D0A6G	0AF60B8C	0B610B6B
5	05630E2A	0E880E4	0E880E4	0E880E4	0E880E4	0E5410E7B	0E5500A7	0D830E06	0E1C0B59
6	052F1010	11B1261	11B1261	1475165A	1475165A	175158B	175158B	15B158B	00011585
7	015B1153E	14D4148A	14D4148A	1486153E	1486153E	17201681	17201681	176A15FA	14311208
8	0PF60E23	0F730ED4	0CDB0D9D	0BDC0A04	0A390RA	0ASD00R97	0DA0D9R9E	0RA20R55	1231386
9	0A90A83	0A690A9A	0A690A9A	0A700A3D	0A700A45	13120A70	0A200A41	0A490A59	133112AD
10	0A250A25	0A360A11	0A970A6D	0A090A0E9	0A3D0B7D	0AOC0A6C	0A590E74	0E1D0A49	0A190A36
11	0A3F0B1F	0A040A45	09EB0D0	0A190A09	0C3D0A9	0A950C4A	0F19162C	032C0030	008C0359
12	03FR57A3	0000001	0000001	000000939	095009AB	09B60A23	0A510E0D	0BA30BAF	0B870FAB
13	0B790A8E	0A10A8C	0B400A69	0A0E0A03	09E90A3E	0994E09B6	09C60A3C	09970A66	0A690A46
14	0C0303D	0A740A31	0A510A2D	0A150A49	0A190A45	0A000AAA	0A590R0A	0A450A65	0A3E0A31
15	0E1C0DDA	0A560A81	0A4750A10	0A480C36	0A820A21	0A8C0G6E	0GDA0A10	0A160B63	0BBD0A8E
16	0C100D55	14B00000	099809C9	09F80A3C	0ABF0B07	0C160C43	0C630C64	10860B80	0C6A0D3F
17	0D970D7D	0D900E08	0E1300000	0E1300000	10CC17F	106119E	124011D9	131A16C	130F1171
18	0ACD0A9	0B000B01	0AAC00B28	0A510A31	0AAC30A31	09FF009F	0AC70A0A	0A960AC3	0A3C0A4D
19	16D615FA	16E1681	16300000	0F5400B37	0D5400B37	0E600B54	0F370D92	0D5400B35	0FC310E
20	132212C2	13AE136E	12D81233	1331018	0F400F97	0E70EC6	0E670E20	0F980E01	0E830E68
21	0D8A0F2A	0F770F2D	0FFF117B	122610EE	10DF0D0F	0F350F7	101D0E4F	0EC30E86	0E530E18
22	0D940E71	0D1770F4C	0D730008	0D970E1C	0D970E1C	0F6112E	0F530F04	0F6511233	13EF1313
23	12B511426	14971347	1453137E	15081116	15A0138E	1400138E	15111347	14971493	15EP11473
24	1CE816FB	17450000	161E1431	12FC1366	1407138E	12F51240	11000EE	0F480FC8	12F51240
25	0D8A0D4E	0A690A9A	0A4D0A4E	0A740A93	0A800A74	0A800A84	0A480A6C	0A480A6C	0A410A41
26	0ABC118D	0A700A6F	0A450A11	0A830A55	0A590A2D	0A9E0A55	0A150A3D	0A3E0A2D	0A460A93
27	0A700A01	0B920A15	0ABC0DB9	10970A29	0A10B1	0A0C0A19	0ID0051	0A8B0A39	0840A31
28	0A000GE	0AEG0B3D	0BBBL0C1B	0BGC0GSE	14E40000	0BBA0D42	0B680BES	0C57006C	0DDE0E2A
29	10A40D25	0DF00CB4	0BB30BDF	0B5E0C06	0BC00CAA	0B990C4D	0A10A0C4D	0A10A0A03	09E209B6
30	09DE0A0A	09BA09BD	0A110A77	0A110A77	0A110B22	0A900B11	0B220BAA	0C450C0C	0E590DE2
31	0F3C0FFB	0F0C1053	11E612E1	11281143	0FFFOFES	0F731026	0E4C0C6	0E980E53	0E080EBC
32	0E8A0D32	0D700D69	0D280DA7	0E150D81	0E040E60	0F17077	112E1053	119E12D8	121913CE
33	13CE1464	12F51410	130B14CB	13CE1558	153514B6	155814D0	15231475	143113CE	145B151A
34	16FB1732	00001615	141012FE	132213CE	136E12C2	1205010B7	0ECA0F2A	0FF9B0E80	0CB10D90
35	0A700A59	0A740A74	0AD30A61	0AAD0A80	0A8400A4D	0A680A80	0A740A8B	0A550A41	0A490A59
36	11830A8E	0A650A49	0A410A6A	0A600A45	0A250A28	0A550A35	0A210A31	0A150A29	0A490A59
37	0A090A4F	0A900A4C	0DFO10F4	0A290A19	0B290A19	0A090E27	0AG80A83	0A410A9E	0A3100E7
38	0D000AE5	0B4000B8R	0BEFB0AA	0C320C000	0000B9556	00000002	00000002	00000002	00000002
39	0BTR0B50	0E200C6D	0CTE0C20	0CTAO0E	0BT700CPA	0E550A0C6	0E750A0E	0E8E0B5E	0CTB05A9
40	0A890A74	0A4D0A62	0A590A58	0A781191	0A700A7C	0A3D0A52	0A070A52	0D2209B0	0AF30A18
41	0A370A28	0A390A9F	0BCC90977	0D660A16	0D6309F7	0DAR0D7	0T980A1D	0A0D0A00	0A170A2D
42	0C600D66	0DEB0E29	0E200DCB8	0D5F0E71	0D190D4F	0F130D04	0D970E18	0DA40D7	0E530FF04
43	104D1186	12F51233	13F51313	12B81420	14971340	14313748	15171418	15A17158E	14D7112E
44	14A21A53	13EE142D	154215EA	16B616EB	12450000	161E1A31	1311135E	1410138E	12E51240
45	04700A74	0A4D0A62	0A590A58	0A781191	0A700A7C	0A3D0A52	0A7C0A3E	0A490A52	0A970A7C
46	0A930A67	0A4D0A62	0A590A58	0A781191	0A700A7C	0A3D0A52	0A490A38	0A4E0A4E	0A270A48
47	0A710A43	0A780A2D	0DDE0A32	0D8A0F26	0F770F2A	1601181	23310EE	10745DD	0F390F5F
48	0C600D66	0DEB0E29	0E200DCB8	0D5F0E71	0D190D4F	0F130D04	0D970E18	0DA40D7	0F71112E
49	0A90A03	0F5E0F9E	0AB4097E	0D900B8D	0A110A79	0A830D08	0A830D08	0A160B25	0A820B8B
50	0C240C0C	0E450C0E	0E600C0E2	0E600C0E2	0F3E0FBF	0F16105C	116120D9	112E1143	0FB083
51	0E9B0A6E	0E0A0E1E	0E600C0E2	0E600C0E2	0E551005C	0D02A0C0A	0D02A0C0A	0D02A0C0A	0D02A0C0A
52	119F12D8	121013CE	120812E53	13CE145B	120914D4	13CE1558	141014D4	14311479	155E140D
53	143113CE	145E151A	15D616B1	16FB1732	0000160C	14101304	132713CE	135E12C2	120710B7
54	0F970F6B	0D800A74	0E600C0E2	0E600C0E2	0D800A74	0D800A74	0D800A74	0D800A74	0D800A74
55	0D9B0A6E	0E0A0E1E	0E600C0E2	0E600C0E2	0E551005C	0D02A0C0A	0D02A0C0A	0D02A0C0A	0D02A0C0A
56	119F12D8	121013CE	120812E53	13CE145B	120914D4	13CE1558	141014D4	14311479	155E140D
57	143113CE	145E151A	15D616B1	16FB1732	0000160C	14101304	132713CE	135E12C2	120710B7
58	0F970F6B	0D800A74	0E600C0E2	0E600C0E2	0D800A74	0D800A74	0D800A74	0D800A74	0D800A74
59	0D9B0A6E	0E0A0E1E	0E600C0E2	0E600C0E2	0E551005C	0D02A0C0A	0D02A0C0A	0D02A0C0A	0D02A0C0A
60	119F12D8	121013CE	120812E53	13CE145B	120914D4	13CE1558	141014D4	14311479	155E140D
61	0F970F6B	0D800A74	0E600C0E2	0E600C0E2	0D800A74	0D800A74	0D800A74	0D800A74	0D800A74